Inorg. Chem. **2003**, *42*, 3549–3558

Synthesis, Structural Investigation, and Solid-State Properties of Iodine-Doped Zirconium Diphthalocyanine, $[ZrPc_2]I_3 \cdot I_2$

Jan Janczak[†]

Institute of Low Temperature and Structure Research, Polish Academy of Sciences, P.O. Box 1410, Okólna 2 str., 50-950 Wrocłw, Poland

Received December 16, 2002

Crystals of iodine-doped zirconium(IV) diphthalocyanine, $[ZrPc_2]I_3 \cdot I_2$ (where Pc = $C_{32}H_{16}N_8$), were grown directly in the reaction of pure zirconium powder with phthalonitrile under a stream of iodine at 260 °C. $[ZrPc_2]I_3 \cdot I_2$ crystallizes in the space group $P2_1/m$ (No. 11) of the monoclinic system with lattice parameters of $a = 6.735(1)$, $b = 25.023(5)$, and $c = 17.440(3)$ Å, $\beta = 99.43(3)°$, and $Z = 2$. The crystals of $[ZrPc_2]I_3 \cdot I_2$ are built up from two pseudo-monodimensional aggregates: one-electron-oxidized $[ZrPc_2]^+$ units; weak interacting triiodide I_3^- ions with neutral diiodine molecules. The I_3^- ions and neutral I_2 molecules in the crystal of $[ZrPc_2]I_3 \cdot I_2$ have been also detected by Raman spectroscopy. The $[ZrPc_2]^+$ units form stacks along the *a* axis, while the polymeric $\cdots I_3^- \cdots I_2 \cdots I_3^- \cdots I_2^- \cdots$ zigzag chains are located in the crystal along the *b* axis, so both pseudo-monodimensional aggregates are perpendicular to each other. This arrangement is different from that found in the tetragonal crystals of $[ZrPc_2](I_3)_{2/3}$ in which both monodimensional aggregates, i.e., the stacks of partially oxidized $[ZrPc_2]^{2/3+}$ units and chains of symmetric triiodide ions, are parallel. EPR experiment together with the X-ray single-crystal analysis clearly shown that oxidation of the diamagnetic $ZrPc_2$ complex by iodine is ligand centered and homogeneously affecting both phthalocyaninato rings of $ZrPc_2$; thus, the formal oxidation state of both Pc rings in $[ZrPc_2]I_3 \cdot I_2$ is nonintegral (–1.5). The UV–vis spectrum of $[ZrPc_2]$ $I_3 \cdot I_2$ is very similar to the spectrum of unoxidized $ZrPc_2$ complex in the B Soret and Q spectral region. However, in the spectrum of $[ZrPc_2]$ $I_3 \cdot I_2$ one additional band at ~502 nm is observed, which indicates the existence of the one-electron-oxidized phthalocyaninato(–) radical ligand and is assigned to the electronic transition from a deeper level to the half-occupied HOMO level. The single-crystal electrical conductivity data show anisotropy and nonmetallic character in conductivity ($d\sigma/dT > 0$). The charge transport mainly proceeds along the pseudo-monodimensional stacks of $[ZrPc_2]^+$ units. The relatively high conductivity along the stacks of one-electron-oxidized $[ZrPc_2]^+$ units results from the staggering orientation of Pc rings (rotation angle 45.0(2)°) that leads to the short inter-ring C_α(pyrrole)–C_α(pyrrole) contacts (2.839(3)–3.024(3) Å). These C_α-pyrrole atoms make appreciable contribution to the partially occupied π-molecular orbital of Pc macrocycle and the greatest overlap of the HOMO orbitals that form the conduction band of partially oxidized molecular crystals.

Introduction

The oxidation by iodine of phthalocyaninato-like metallomacrocyclic complexes has yielded several number of one-dimensional highly conducting materials.[1−12] The most extensively characterized compound in this series is iodine-doped (phthalocyaninato)nickel(II), NiPcI,[13−18] the first low-temperature molecular conductor with the conductivity of

[†] E-mail: janczak@int.pan.wroc.pl. Tel.: +48-71-343-5021. Fax: +48-71-441-029.

(1) Martinsen, J.; Pace, L. J.; Phillips, T. E.; Hoffman, B. M.; Ibers, J. A. *J. Am. Chem. Soc.* **1982**, *104*, 83−91.
(2) Phillips, T. E.; Scaringe, R. P.; Hoffman, B. M.; Ibers, J. A. *J. Am. Chem. Soc.* **1980**, *102*, 3435−3444.
(3) Phillips, T. E.; Hoffman, B. M. *J. Am. Chem. Soc.* **1977**, *99*, 7734−7736.
(4) Ibers, J. A.; Pace, L. J.; Martinsen, J.; Hoffman, B. M. *Struct. Bonding (Berlin)* **1982**, *50*, 1−55.
(5) Hoffman, B. M.; Ibers, J. A. *Acc. Chem. Res.* **1983**, *16*, 15−21.
(6) Hoffman, B. M.; Martinsen, J.; Pace, L. J.; Ibers, J. A. In *Extended Linear Chain Compounds*; Miller, J. S., Ed.; Plenum: New York, 1983; Vol. 3, pp 459−549.
(7) Palmer, S. M.; Stanton, J. L.; Martinsen, J.; Ogawa, M. Y.; Heuer, W. B. Van Wallendael, S. E.; Hoffman, B. M.; Ibers, J. A. *Mol. Cryst. Liq. Cryst.* **1985**, *125*, 1−11.
(8) Marks, T. J. *Science* **1985**, *227*, 881−889.
(9) Liou, K.; Ogawa, M. Y.; Newcomb, T. P.; Quirion, G.; Lec, M.; Poirier, M.; Halperin, W. P.; Hoffman, B. M.; Ibers, J. A. *Inorg. Chem.* **1989**, *28*, 3889−3896.

10.1021/ic020717i CCC: $25.00
Published on Web 05/03/2003

Scheme 1

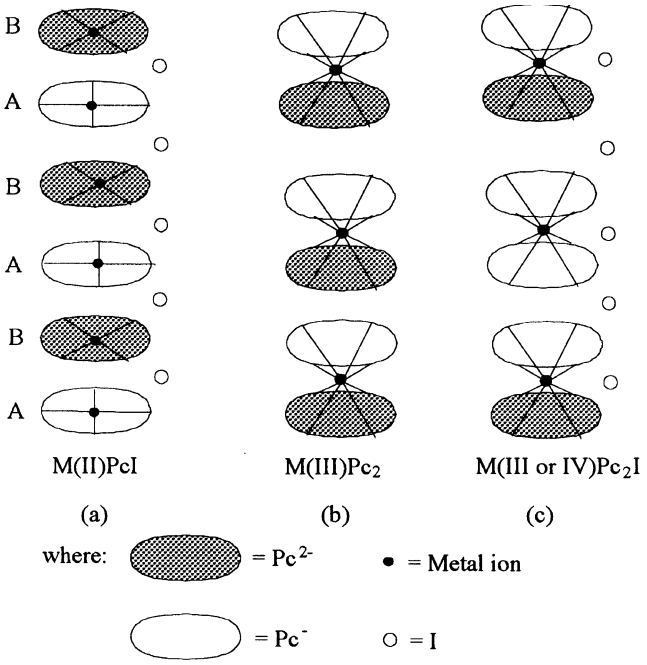

ca. 600 Ω^{-1} cm^{-1} at the ambient temperature.[15] The majority of the partially oxidized by iodine metallophthalocyaninato complexes crystallize in the tetragonal system. A single structural motif was retained throughout this series of materials that consists of metal-over-metal columnar stacks of partially oxidized $MPc^{\delta+}$ units surrounded by chains of triiodide (I_3^-) ions. The arrangements of the metallomacrocycles in the pseudo-monodimensional stacks can be described by an alternate ABAB pattern along the *c*-axis (Scheme 1a) with the rotation angles of about 40° between the A and B macrocycles (B is related to A by a symmetry), the interplanar spacing between the macrocycles within the stacks being not too different from the average value of ~3.25 Å, which indicates a strong $\pi-\pi$ interaction between the macrocyclic rings along the stack. This interaction is responsible for the observed high conductivity of these materials. Extensive theoretical and experimental investigations predict the highest conductivity in these systems when the rotation angle of macrocycles is equal to 45°; this angle provides the greatest overlap of the a_{1u} HOMO π-orbitals of the macrocycle.[19,20]

The iodine part of these metallophthalocyaninato materials is usually disordered, as indicated by the presence of the diffuse X-ray scattering in the planes perpendicular to the stacking direction.[21−23] An analysis of the diffuse scattering lines that could be indexed on the basis of the superlattice spacing of 9.5−9.8 Å indicates for the ordered chains of the symmetrical triiodide ions, I_3^-, which are disordered (translated) with respect to their neighbors.[15,24]

Understanding of the charge transport in these partially oxidized materials requires the knowledge of a number of characteristic of the materials such as composition, structure, and the "ionicity", i.e., the degree of the partial oxidation. Resonance Raman and ^{129}I Mössbauer spectroscopy offer a simple means of characterizing the polyiodide species and determining the "ionicity".[25−27] The EPR measurements are useful for characterizing the partially oxidized complexes in which both the central metal ion such as Mn, Fe, or Co and the π-macrocyclic ring can be redox active, since both oxidized forms $M^{2+}(Pc^{\bullet-})I$ and $M^{3+}(Pc^{2-})I$ exhibit different EPR spectra.[28] Additionally, EPR measurements provide clear evidence for the exchange coupling between the localized unpaired electron on the central metal ions and the π-carriers of macrocycle within the stacks as was observed for the CoPcI [29] and CuPcI,[30] both linear-chain metal-spine conductors.

Partially oxidized metallodiphthalocyaninato complexes are less studied.[31] This family is divided into two categories: (1) undoped metal(III) diphthalocyanines (Scheme 1b);[32−37] (2) iodine-doped partially oxidized metal(III) and

(10) Rende, D. E.; Heagy, M. D.; Heuer, W. B.; Liou, K.; Thompson, J. A. Hoffman, B. M.; Musselman, R. L. *Inorg. Chem.* **1992**, *31*, 352−358.
(11) Marks, T. J. *Angew. Chem., Int. Ed. Engl.* **1990**, *29*, 857−879.
(12) Miller, D. C.; Bollinger, J. C.; Hoffman, B. M.; Ibers, J. A. *Inorg. Chem.* **1994**, *33*, 3354−3357.
(13) Petersen, J. L.; Schramm, C. J.; Stojakovic, D. R.; Hoffman, B. M.; Marks, T. J. *J. Am. Chem. Soc.* **1977**, *99*, 286−288.
(14) Schramm, C. J.; Stojakovic, D. R. Hoffman, B. M.; Marks, T. J. *Science* **1978**, *200*, 47−48.
(15) Schramm, C. J.; Scaringe, R. P.; Stojakovic, D. R.; Hoffman, B. M.; Ibers, J. A.; Marks, T. J. *J. Am. Chem. Soc.* **1980**, *102*, 6702−6713.
(16) Martinsen, J.; Greene, R. L.; Palmer, S. M.; Hoffman, B. M. *J. Am. Chem. Soc.* **1983**, *105*, 677−678.
(17) Martinsen, J.; Tanaka, J.; Greene, R. L.; Hoffman, B. M. *Phys. Rev. B: Condens. Matter* **1984**, *30*, 6296−6276.
(18) Palmer, S. M.; Ogawa, M. Y.; Martinsen, J.; Stanton, J. L.; Hoffman, B. M.; Ibers, J. A. Greene, R. L. *Mol. Cryst. Liq. Cryst.* **1985**, *120*, 427−432.
(19) Pace, L. J.; Martinsen, J.; Ulman, A.; Hoffman, B. M.; Ibers, J. A. *J. Am. Chem. Soc.* **1983**, *105*, 2612−2620.
(20) Pietro, W. J.; Marks, T. J.; Ratner, M. A. *J. Am. Chem. Soc.* **1985**, *107*, 5387−5391.
(21) Cowie, M.; Gleizes, A.; Grynkiewich, G. W.; Kalina, D. W.; McClure, M. S.; Scaringe, R. P.; Teitelbaum, R. C.; Ruby, S. L.; Ibers, J. A. Kannweurf, C. R. *J. Am. Chem. Soc.* **1979**, *101*, 2921−2936.
(22) Enders, H.; Keller, H. J.; Megnamisi-Belombe, M.; Moroni, W.; Pritzkow, H.; Weiss, J.; Gomes, R. *Acta Crystallogr., Sect. A* **1976**, *32*, 954−957.
(23) Scaringe, R. P.; Ibers, J. A. *Acta Crystallogr., Sect. A* **1979**, 803−810.
(24) Euler, W. B.; Martinsen, J. Pace, L. J.; Hoffman, B. M.; Ibers, J. A. *Mol. Cryst. Liq. Cryst.* **1982**, *81*, 231−242.
(25) Teitelbaum, R. C.; Ruby, S. L.; Marks, T. J. *J. Am. Chem. Soc*. **1978**, *100*, 3215−3217.
(26) Teitelbaum, R. C.; Ruby, S. L.; Marks, T. J. *J. Am. Chem. Soc*. **1980**, *102*, 3222−3228.
(27) Mizuno, M.; Tanaka, J.; Harada, I. *J. Phys. Chem.* **1981**, *85*, 1789−1794.
(28) *Phthalocyanines: Properties and Applications*; Lenzoff, C. C., Lever, A. B. P., Eds.; VCH Publishers: New York, 1989−1996; Vols. 1−4.
(29) Martinsen, J.; Stanton, J. L.; Greene, R. L.; Tanaka, J.; Hoffman, B. M.; Ibers, J. A. *J. Am. Chem. Soc.* **1985**, *107*, 6915−6920.
(30) Ogawa, M. Y.; Martinsen, J.; Palmer, S. M.; Stanton, J. L.; Tanaka, J.; Greene, R, L.; Hoffman, B. M. Ibers, J. A. *J. Am. Chem. Soc.* **1987**, *109*, 1115−1121.
(31) Kubiak, R.; Janczak, J. *Cryst. Res. Technol.* **2001**, *36*, 1095−1104.
(32) Darovsky, A.; Wu, L. Y.; Lee, P.; Shen, H. S. *Acta Crystallogr., Sect. C* **1991**, *47*, 1836−1838.
(33) Darovsky, A.; Keserashvili, V.; Harlow, R.; Mutikainen, I. *Acta Crystallogr., Sect. B* **1994**, *50*, 582−588.
(34) Moussavi, M.; DeCian, A.; Fischer, J.; Weiss, R. *Inorg. Chem.* **1988**, *27*, 1287−1291.
(35) Chabach, D.; Lachbar, M.; DeCian, A.; Fischer, J.; Weiss, R. *New J. Chem.* **1992**, *16*, 431−437.
(36) Ostendorph, G.; Werner, J. P.; Homborg, H. *Acta Crystallogr., Sect. C* **1995**, *51*, 1125−1128.
(37) Janczak, J.; Kubiak, R.; Jezierski, A. *Inorg. Chem.* **1995**, *34*, 3505−3509.

metal(IV) diphthalocyanines (Scheme 1c).[38−43] In the first category, $M^{III}Pc_2$, exhibiting semiconducting properties, the trivalent metal ion is surrounded by two different phthalocyaninato ligands: Pc^{2-}; one-oxidized $Pc^{\bullet-}$ radical ion. For example, the magnetic susceptibility measurement of the $InPc_2$ complex with one unpaired electron shows its paramagnetic character and the unpaired electron is localized on a Pc ring as indicated by EPR spectroscopy.[37] However, the X-ray single-crystal structure analysis shows that both halves of this sandwich-type complexes are equivalent structurally; thus, the nonintegral oxidation state should be assigned to either of them ($\rho = -1.5$). In the second category, iodine-doped metal(III) and metal(IV) diphthalocyanines, the conductivity depends strongly on the amount of the iodine-doped atoms, which is closely correlated with the formal oxidation state of the macrocyclic rings. For example, the oxidation state of Pc rings in the two $[UPc_2]I_{5/3}$ and $[UPc_2]I_2$ is equal to -1.722 and -1.667, respectively,[40,42] since in both complexes the iodine-doped atoms exist in the triiodide form I_3^-. The further oxidation of above-mentioned semiconducting metallodiphthalocyaninato complexes leads to the Mott−Hubbard isolator in which, similar to lithium phthalocyanine (LiPc), the formal oxidation state of the Pc rings is equal to -1.

Recently, we have reported the synthesis, structure, and some properties of a new iodine-doped complex with the composition of $[YbPc_2]I_2$ and $[AsPc_2]I_2$.[41] Although the As complex possesses the same general formula as other metallodiphthalocyaninato complexes, MPc_2I_2, the X-ray and EPR investigations clearly show that the crystals of the iodine-doped As−phthalocyaninato complex are built up from two different partially oxidized components: the arsenic phthalocyaninato (AsPc) and phthalocyanine units; linear chains of symmetrical triiodide ions.[41]

Using a slightly modified method[44] we have obtained several iodine-doped metallophthalocyanines. Additionally, it has been stated that depending on the reaction conditions and the metal used in the synthesis, the iodine atoms can be directly bonded to the central metal cation yielding mono-[45−47] and diiodometallophthalocyanines (cis or trans position).[48−50] Moreover, the iodine-doped atoms can form the neutral I_2 molecules as bridge molecules for dimerization of monoiodophthalocyanines[51] or for developing a polymeric structure of diiodometallophthalocyanines.[52,53]

Similar to iodine-doped metallomonophthalocyanines the iodine-doped sandwich-type diphthalocyaninato complexes also crystallize in the tetragonal system. However, this iodine-doped zirconium diphthalocyanine complex crystallize in the monoclinic system, so it not isostructural with the known $[MPc_2]I_x$ complexes. Additionally, the index of iodine atoms in the $[ZrPc_2]I_5$ complex investigated here is more than 2 times greater in relation to that observed in other diphthalocyaninato complexes: $[TiPc_2]I_2$,[38] $[BiPc_2]I_{3/2}$,[39] $[UPc_2]I_{5/3}$,[40] $[YbPc_2]I_2$,[41] $[UPc_2]I_2$,[42] and $[InPc_2]I_2$ and $[ZrPc_2]I_2$.[43] Herein we report the synthesis, characterization, and crystal structure of the $[ZrPc_2]I_5$ complex. Additionally, the correlation between the structure and properties of the monoclinic $[ZrPc_2]I_5$ and the tetragonal $[ZrPc_2]I_2$ complexes[43] has been discussed.

Experimental Section

Synthesis. All reagents were of the highest grade commercially available and were used as received. The crystals of $[ZrPc_2]I_3{\cdot}I_2$ were obtained directly by the reaction of the pure powdered zirconium and 1,2-dicyanobenzene under a stream of iodine. The powdered zirconium (0.2 g), 1,2-dicyanobenzene (2.26 g), and iodine (1.44 g) in a molar proportion of 1:8:5, with about 5% excess of iodine, were mixed together and pressed into pellets. The pellets were inserted into an evacuated glass ampule and sealed. The ampule was heated at 260 °C for 12 h. At this temperature (260 °C), the liquid 1,2-dicyanobenzene undergoes catalytic tetramerization forming the phthalocyaninato macroring, which accepts the electrons from zirconium forming the $ZrPc_2$ complex. Simultaneously, the iodine atoms (as oxidant) partially oxidized the $ZrPc_2$ molecules yielding good quality black-violet single crystals of $[ZrPc_2]I_3{\cdot}I_2$ (Scheme 2). The elemental analysis was carried out on an energy dispersive spectrometer. Anal. Found: C, 43.21; N, 12.84; Zr, 5.29; I, 36.84; H, 1.82. Calcd for $C_{64}H_{32}N_{16}ZrI_5$: C, 43.91; N, 12.79; Zr, 5.23; I, 36.25; H, 1.84.

X-ray Data Collection and Structure Determination. The X-ray single-crystal data were collected on a KUMA KM-4 diffractometer equipped with a two-dimensional area CCD detector on the single crystal with dimensions of $0.24 \times 0.22 \times 0.18$ mm. Graphite-monochromatized Mo Kα radiation ($\lambda = 0.710\,73$ Å) and the ω-scan technique with the $\Delta\omega = 0.75°$ for one image were used. A total of 960 images for six different runs covering over 95% of the Ewald sphere were performed. The cell parameters were refined by the least-squares method on the basis of all reflections with $F^2 > 2\sigma(F^2)$. One image was monitored as a standard after every 40 images for control the stability of the crystal. Integration of the intensities and correction for Lorentz and polarization effects were performed using a KUMA KM-4 CCD software.[54] Face-indexed analytical absorption was calculated using the SHELXTL program.[55] The minimum and maximum transmission factors are 0.5418 and 06224, respectively. A total 22 932 (6527 independent,

(38) Copabianchi, A.; Ercolani, C.; Paoletti, A. M.; Pennesi, G.; Rossi, G.; Chiesi-Villa, A.; Rizzoli, C. *Inorg. Chem.* **1993**, *32*, 4605−4611.
(39) Janczak, J.; Kubiak, R.; Hahn, F. *Inorg. Chim. Acta* **1998**, *281*, 195−200.
(40) Janczak, J.; Kubiak, R. *Polyhedron* **1999**, *18*, 1621−1627.
(41) Janczak, J.; Kubiak, R.; Jezierski, A. *Inorg. Chem.* **1999**, *38*, 2043−2049.
(42) Janczak, J.; Kubiak, R.; Svoboda, I.; Jezierski, A.; Fuess, H. *Inorg. Chim. Acta* **2000**, *304*, 150−155.
(43) Janczak, J.; Idemori, Y. M. *Inorg. Chim. Acta* **2001**, *325*, 85−93.
(44) Kubiak, R.; Janczak, J. *J. Alloys Compd.* **1993**, *200*, L7−L8.
(45) Janczak, J.; Kubiak, R. *Inorg. Chim. Acta* **1999**, *288*, 174−180.
(46) Janczak, J.; Idemori, Y. M. *Acta Crystallogr., Sect. C* **2001**, *57*, 924−925.
(47) Schweiger, K.; Hückstadt, H.; Homborg, H. *Z. Anorg. Allg. Chem.* **1998**, *624*, 167−169.
(48) Kubiak, R.; Ejsmont, K. *Acta Crystallogr., Sect. C* **1997**, *53*, 1051−1054.
(49) Kubiak, R.; Ejsmont, K. *Acta Crystallogr., Sect. C* **1998**, *54*, 1844−1846.
(50) Janczak, J.; Kubiak, R. *Pol. J. Chem.* **1999**, *73*, 1587−1592.
(51) Janczak, J.; Kubiak, R.; Hahn, F. *Inorg. Chim. Acta* **1999**, *287*, 101−104.
(52) Janczak, J.; Razik, M.; Kubiak, R. *Acta Crystallogr., Sect. C* **1999**, *55*, 359−361.
(53) Janczak, J.; Idemori, Y. M. *Inorg. Chem.* **2002**, *41*, 5059−5065.
(54) *KUMA Diffraction, KUMA KM-4 CCD program package*, Ver. 163; KUMA: Wrocław, Poland, 2000.
(55) Sheldrick, G. M. *SHELXTL Program*; Siemens Analytical X-ray Instrument Inc.: Madison, WI, 1991.

Scheme 2

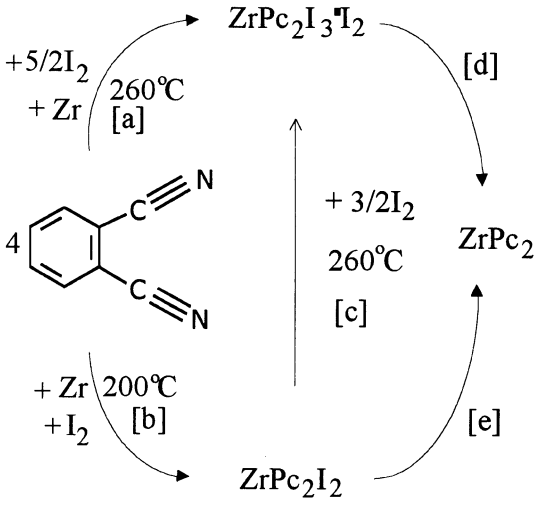

where Pc =

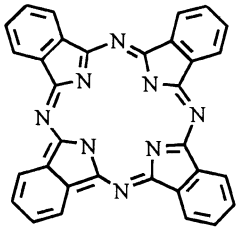

$R_{int} = 0.0185$) reflections were integrated and used for the crystal structure determination. The structure was solved by the Patterson heavy atom method and refined by the full-matrix least-squares methods using the SHELXL97 program[56] with anisotropic thermal parameters for all non-hydrogen atoms. The hydrogen atoms of the phenyl rings were introduced in their computed coordinates (HFIX 43) with isotropic thermal parameters $U_{iso}(H) = 1.2U_{iso}$(C), i.e., 20% higher than the thermal parameter of the carbon atom directly bonded the H atom. The final difference Fourier maps showed no peaks of chemically significance (+0.670 and −0.342 e Å^{-3}). More details of data collection and final refinement parameters are listed in the Table 1 and in the Supporting Information. Selected bond lengths and angles are summarized in Table 2.

UV−Vis Spectroscopy. Measurements of the electronic spectra of $[ZrPc_2]I_3 \cdot I_2$ and $ZrPc_2$ were carried out at room temperature using a Cary-Varian 2300 spectrometer. The UV−vis spectra were recorded on a thin solid film between the quartz glass prepared from Nujol mulls since the thin solid film of the $[ZrPc_2]I_3 \cdot I_2$ complex by sublimation in a vacuum was unable to be prepared due to decomposition to $ZrPc_2$ and I_2.

Raman Spectroscopy. The Raman spectrum of a microcrystalline sample was recorded at room temperature on a Jobin-Yvon Ramanor U-1000 spectrometer equipped with a photomultiplier type detector and phonon-counting hardware. The 90° geometry was used. An argon-ion laser line at 514.5 nm of power 100 mW was used as exciting radiation. Resolution was set up to 3 cm^{-1}.

Magnetic Susceptibility Measurement. Magnetic susceptibility measurement of $[ZrPc_2]I_3 \cdot I_2$ was carried out on a polycrystalline sample in the temperature range 2−300 K with a Quantum Design SQUID magnetometer (San Diego, CA). The susceptometer was calibrated with HgCo(SCN) and $(NH_4)_2Mn(SO_4)_2 \cdot 12H_2O$. Data were recorded at the magnetic field of 0.5 T on a sample of 60 mg.

Electron Paramagnetic Resonance Spectroscopy. EPR measurements were made on SE-Radiopan and ESR 300E-Bruker X-band spectrometers at room temperature. The studies were carried out on solid samples of 2−5 mg. The concentrations of the free radicals in the samples of $[ZrPc_2]I_3 \cdot I_2$ were calculated using standard integration of the derivative signal and by comparing the area with the area determined with the free radical standards (DPPH, TEMPO, TEMPOL, and Rickitt's ultramarine were used as standards). One EPR strong signal at $g = 2.0026$ with a bandwidth of $\Gamma = 6.2$ G was observed.

Single-Crystal Electrical Conductivity Measurements. Single crystals of $[ZrPc_2]I_3 \cdot I_2$ were mounted on silvered graphite fibbers, and electrical contact was made with a palladium paste. The conductivity measurements were performed along the *a* and *b* axes, i.e., along the stacks of partially oxidized $[ZrPc_2]$ units and along the polyiodide $\cdots I_3^- \cdots I_2 \cdots I_3^- \cdots I_2 \cdots$ zigzag chains using a standard four-point probe technique[57] with a sampling current of 20 μA. Variation of the temperature was archived by placing the samples in a cold-gas stream (N_2 or He). The conductivity of the material

Table 1. Crystallographic Data and Final Refinement Parameters for $[ZrPc_2]I_3 \cdot I_2$

chem formula	$C_{64}H_{32}N_{16}ZrI_5$
M_r	1750.78
temp/°C	295(2)
cryst system	monoclinic
space group	$P2_1/m$ (No. 11)
unit cell dimens	
a, *b*, *c*/Å	6.735(1), 25.023(5), 17.440(3)
β /deg	99.43(3)
V/Å^3	2899.4(9)
Z	2
D_{obs} (measd by flotation)/g cm^{-3}	2.00
D_{calc}/g cm^{-3}	2.005
radiation, Mo Kα/Å	0.710 73
abs coeff, μ/mm^{-1}	2.910
refinement on F^2	0.0483
R [$F^2 > 2\sigma(F^2)$][a]	
wR (F^2 all reflcns)[b]	0.0573
Goodness-of-fit, *S*	1.012
Resid electron density, $\Delta\rho_{max}$, $\Delta\rho_{min}$/e Å^{-3}	+0.670, −0.342

[a] $R = \sum||F_o| - ||F_c||/\sum F_o$. [b] $wR = \{\sum[w(F_o^2 - F_c^2)^2]/\sum wF_o^4\}^{1/2}$; $w^{-1} = \sigma^2(F_o^2) + (0.0217P)^2$, where $P = (F_o^2 + 2F_c^2)/3$.

Table 2. Selected Bond Distance (Å) and Angles (deg) for $[ZrPc_2]I_3 \cdot I_2$ [a]

I1−I2	2.9234(7)	I1−I2^{i}	2.9234(7)
I2−I3	3.548(1)	I3−I3^{ii}	2.7365(10)
Zr−N2	2.278(3)	Zr−N4	2.299(3)
Zr−N6	2.292(4)	Zr−N8	2.312(3)
Zr−N10	2.331(4)		
I2−I1−I2^{i}	175.50(3)	I1−I2−I3	132.52(2)
I2−I3−I3^{ii}	169.64(3)	N2−Zr−N4	73.0(1)
N2−Zr−N6	80.3(1)	N2−Zr−N8	78.7(1)
N2−Zr−N2^{i}	72.8(1)	N4−Zr−N2^{i}	113.99(9)
N4−Zr−N6	143.37(7)	N4−Zr−N8	77.1(1)
N4−Zr−N10	76.5(1)	N6−Zr−N10	113.8(1)
N8−Zr−N10	72.77(9)	N2−Zr−N10	142.00(7)
N6−Zr−N8	73.37(9)	N4−Zr−N8^{i}	140.5(1)
N2−Zr−N8^{i}	143.9(1)	N4−Zr−N4^{i}	72.1(1)
N8−Zr−N8^{I}	115.5(1)		

[a] Symmetry code: i = *x*, 1/2 − y, *z*; ii = −*x*, 1 − *y*, 1 − *z*.

(56) Sheldrick, G. M. *SHELXL-97, Program for the Solution and Refinement of Crystal Structures*; University of Göttingen: Göttingen, Germany, 1997.

(57) Phillips, T. E.; Anderson, J. R.; Schramm, C. J.; Hoffman, B. M. *Rev. Sci. Instrum.* **1979**, *50*, 263−265.

was calculated from the relationship $\sigma = L/RA$, where σ is the conductivity (in Ω^{-1} cm^{-1}), R is the measured resistance (in Ω) of the material between two inner contacts, L is the separation distance between two inner contacts (in cm), and A is the cross-sectional area of the sample (in cm^2). For the conductivity measurement was selected a single crystal with a dimension of 1.124 mm (along the crystallographic *a* axis), 0.325 mm (along the *c* axis), and 0.168 mm along the *b* axis. Estimated uncertainty in these measurements is about 1×10^{-3} mm. The area A was estimated from the maximum cross-sectional distance as observed with a microscope. An empirical analysis of the measurement errors indicates that the area is uncertain by $\delta A/A \approx \pm 0.2$, leading to an uncertainty $\Delta\sigma/\sigma \approx \pm 0.3$. The measurements were repeated on several (eight) single crystals with different dimensions (0.50−1.10 mm along the *a* axis, 0.122−0.352 mm along the *b* axis, and 0.062−0.216 mm along the *c* axis). The differences in the measured conductivities on these single crystals are ≈±5%.

Results and Discussion

Synthesis and Characterization. The crystals of $[ZrPc_2]I_3{\cdot}I_2$ have been directly obtained from pure powdered zirconium and phthalonitrile under a stream of iodine at 260 °C (see Scheme 2, step a). Earlier, it has been reported that the reaction of powdered zirconium with phthalonitrile and iodine at lower temperature (∼200 °C) yields the tetragonal crystals of $[ZrPc_2]I_2$ (Scheme 2, step b).[43] The crystals of the $[ZrPc_2]I_3{\cdot}I_2$ complex at this lower temperature (∼200 °C) could not be obtained; thus, undoubtedly the higher temperature (260 °C) is conducive to formation of this complex. The $[ZrPc_2]I_3{\cdot}I_2$ complex could be also obtained from $[ZrPc_2]I_2$ by the prolonged temperature process at 260 °C under an iodine stream (see Scheme 2, step c) but only in powdered form (identified by elemental analysis and X-ray powder diffraction experiment). Both crystals of iodine-doped zirconium diphthalocyaninine, tetragonal $[ZrPc_2]I_2$ and monoclinic $[ZrPc_2]I_3{\cdot}I_2$, under vacuum and at higher temperature after several hours lose the iodine atoms yielding the known zirconium diphthalocyanine, $ZrPc_2$ (see Scheme 2, steps d and e).[58,59] The $[ZrPc_2]I_3{\cdot}I_2$ complex is not soluble in water, methanol, or ethanol and is slightly soluble in dichloromethane, DMF, DMSO, pyridine, and in other aromatic solvent like chloronaphthalene or quinoline. However, from the solution after 4−5 weeks black powder material was obtained. The elemental analysis of this black powder material is consistent with the composition of $ZrPc_2$. Thus in the solution the decomposition process of $[ZrPc_2]I_3{\cdot}I_2$ complex into the $ZrPc_2$ and iodine takes place. The decomposition of this complex in solution depends strongly on the temperature and takes place several times quicker in hot solvents. Contact of the $[ZrPc_2]I_3{\cdot}I_2$ complex with dilute acid (H_2SO_4, HNO_3) leads to the demetalation yielding the α-form of metal-free phthalocyanine (α-H_2Pc)[60] and appropriate salt.

Resonance Raman Spectroscopy. Determination of the stoichiometric formula $[ZrPc_2]I_5$ by chemical analysis gives no information about the charge on the macrocyclic rings, i.e., "ionicity", since iodine-doped atoms can assume a variety forms in the crystal as I_2, I^-, I_3^-, I_4^{2-}, I_5^-, etc. To relate the charge transport properties of $[ZrPc_2]I_5$ to the degree of the oxidation by iodine of the $[ZrPc_2]^{\delta+}$ unit, the form of the iodine must be determined. Resonance Raman spectroscopy is particularly useful for the identification of the iodine forms in the sample. The resonance Raman spectrum measured on the polycrystalline sample at room temperature (see Figure 1) exhibits two sharp strong fundamental bands. One fundamental absorption band at about 109 cm^{-1} with characteristic progression of bands at ∼220 and ∼330 cm^{-1} is typical for the sample containing the triiodide I_3^- ions.[25−27] The second fundamental absorption band at ∼185 cm^{-1} shows the expected vibrational band of the neutral I_2 molecule that interacts weakly with the I_3^- ions.[25,26] The absence of any peaks at ∼160 cm^{-1} eliminates I_5^- ion as a predominant iodine form.[25−27] This conclusion is fully consistent with the X-ray structure analysis; thus, the complex $[ZrPc_2]I_5$ should be written as $[ZrPc_2]I_3{\cdot}I_2$.

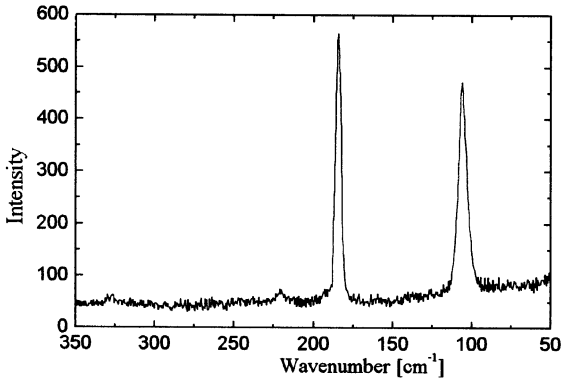

Figure 1. Resonance Raman spectrum of polycrystalline sample of $[ZrPc_2]I_3{\cdot}I_2$.

Description of the Structure. The crystals of $[ZrPc_2]I_3{\cdot}I_2$ are built up from partially oxidized $[ZrPc_2]^+$ units, triiodide ions, and neutral diiodine molecules. The one-electron-oxidized $[ZrPc_2]^+$ sandwich unit is located on the special position in the crystal, and therefore it has *m* symmetry. The central closed-shell Zr^{4+} cation (d^0 configuration) is eight coordinated by two saucer-shaped phthalocyaninato units (see Figure 2), Pc^{2-} and one-electron-oxidized $Pc^{\bullet-}$ radical form (identified by EPR spectroscopy). However, the Zr^{4+} cation is located at the center of the Pc rings with a distance of 1.247(3) Å from both N_4-isoindole planes. Thus, the Zr^{4+} cation equally interacts with both Pc rings; therefore, it should be stated that both phthalocyaninato macrorings are equivalent and should be assigned the nonintegral oxidation state of −1.5 to both of them. Both phthalocyaninato macrocyclic ligands of $[ZrPc_2]^+$ unit are appreciably deviated from the weighted least-squares plane defined by four N-isoindole atoms. The largest deviations from the N_4-isoindole plane (without the H atoms) are observed for the outermost carbon atoms of the phenyl rings, for example C12, 1.305(3) Å, and C13, 1.099(3) Å, for one phthalocyaninato ring and C17, 1.073(3) Å, and C18, 0.893(3) Å, for the second ring. The distortion of the phthalocyaninato rings from planarity in the crystal of $[ZrPc_2]I_3{\cdot}I_2$ is smaller than

(58) Silver, J.; Lukes, P. J.; Hey, P. K.; O'Connor, J. M. *Polyhedron* **1989**, *8*, 1631−1635.
(59) Silver, J.; Lukes, J. P.; Howe, S. D.; Howlin, B. *J. Mater. Chem.* **1991**, *1*, 29−35.
(60) Janczak, J. *Pol. J. Chem.* **2000**, *74*, 157−162.

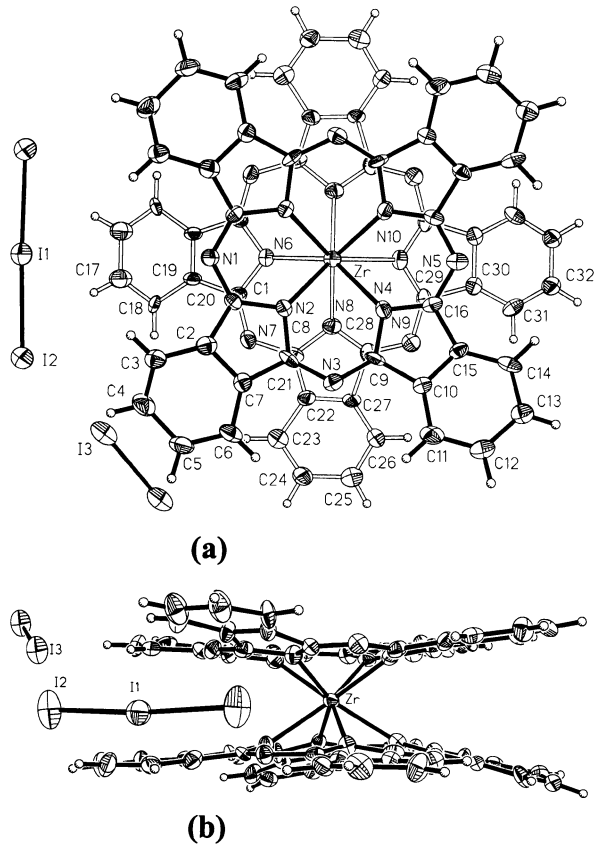

Figure 2. View of the $[ZrPc_2]I_3{\cdot}I_2$. molecule with labeling scheme: (a) top view; (b) side view. Displacement ellipsoids are shown at the 50% probability level.

in the crystal of unoxidized $ZrPc_2$, in which the greatest deviation equals 1.47 Å.[59] Comparison of the displacements of the outermost carbon atoms for some metallodiphthalocyaninato structures[61−65] is collected in Table 3. As can be seen from the data collected in Table 3, both zirconium structures, $ZrPc_2$ and one-electron-oxidized $[ZrPc_2]I_3{\cdot}I_2$, contain the most deviated phthalocyaninato macrorings. The Zr−N distances in the $[ZrPc_2]^+$ unit are ranging from 2.279(3) to 2.328(3) Å, and they are slightly shorter than those observed in the crystal of unoxidized $ZrPc_2$ complex.[58] This is likely due to the weaker repulsion interaction between the Pc^{2-} and $Pc^{\bullet-}$ rings in relation to $ZrPc_2$ in which this $Pc^{2-}\cdots Pc^{2-}$ interaction is undoubtedly greater. The M−N distances in zirconium diphthalocyaninato complexes are shorter than those of the other known sandwich-type diphthalocyaninato structures due to the relatively small Zr^{4+} cation.[66] The effect of the small radius of Zr^{4+} cation and its great formal oxidation state is that the phthalocyaninato rings are located closer to the Zr^{4+} cation and the distance between N_4-N_4 isoindole planes is the shortest within the known sandwich-type diphthalocyaninato structures (see Table 4). This is the reason for the mostly buckle form of the Pc-ring system. The Pc rings in $[ZrPc_2]I_3{\cdot}I_2$ are staggered at an angle of 45.0(2)°, and this is an additional reason for the closer location of the Pc rings in relation to the unoxidized $ZrPc_2$ in which the rotation angle is equal to 42°.[59] The close proximity of the N_4-planes indicates the interaction of the π-clouds and adds to the distortion of the rest of the Pc rings from the N_4-isoindole planes. The staggered orientation of the Pc rings give the square antiprismatic coordination of the central Zr^{4+} cation and, as can be seen from Figure 2, indicates that the outermost carbon atoms of the six-membered carbon rings are apart as for noninterpenetrating π-clouds. In the second crystal of partially oxidized zirconium diphthalocayanine, $[ZrPc_2](I_3)_{2/3}$, the relatively large N_4-N_4 interplanar distance is due to the symmetry of the crystal (tetragonal system, space group *P4*/*mcc*) and to the fact that both Pc rings are symmetrically equivalent and located at the special position in the crystal (on the crystallographic *m* plane).[43] As can be seen from Table 4, the shortest N_4-N_4 distance of 2.32 Å is observed in the crystal of $TiPc_2$;[64] however, this complex belongs to the new family of sandwiched metallodiphthalocyanines in which the

Table 3. Comparison of the Displacements of the Outermost Carbon Atoms of Phenyl Rings from the N_4-Isoindole Plane in the Metallodiphthalocyanine (MPc_2) Structures

	displacement of the phenyl ring C atoms from the N4-isoindole plane (Å)		
compd	least displaced	most displaced	ref
$ZrPc_2$	0.49	1.47	55
$[ZrPc_2]I_3{\cdot}I_2$	0.394 (C4)	0.465 (C5)	this work
	1.099 (C13)	1.305 (C12)	
	0.541 (C24)	0.653 (C25)	
	0.677 (C32)	1.073 (C17)	
$[ZrPc_2](I_3)_{2/3}$ [a]	0	0	43
UPc_2	0.48	1.10	57
α-$SnPc_2$	0.18	1.01	58
β-$SnPc_2$	0.25	1.21	61
$Ln^{III}Pc_2$	0.25	1.10	59
$TiPc_2$ [b]	1.06	1.94	60
$[TiPc_2](I_3)_{2/3}$	0.61	0.67	38
$[UPc_2](I_3)_{5/9}$ [a]	0	0	40
$[UPc_2](I_3)_{2/3}$	0.083	0.335	42
In(III)Pc2	0.12	0.88	37
$[In^{III}Pc_2](I_3)_{2/3}$ [a]	0	0	43

[a] Pc rings are closely planar. [b] "Stapled" by two C−C σ bonds.

Table 4. Comparison of the Coordination of the Central Metal Ion of MPc_2 Structures

compd	formal oxidn state of Pc ring	av M−N bond dist (Å)	dist between N4−N4 plane (Å)	staggering angle (deg)	ref
$ZrPc_2$	−2	2.30	2.52	42	55
$[ZrPc_2]I_3{\cdot}I_2$	−1.5	2.297	2.494(3)	45.0(2)	this work
$[ZrPc_2](I_3)_{2/3}$	−1.667	2.527	3.244(3)	40.6(2)	43
Upc_2	−2	2.43	2.81	37	57
$[UPc_2](I_3)_{5/9}$	−1.667	2.448	2.903(5)	40.2(6)	42
$[UPc_2](I_3)_{2/3}$	−1.772	2.549	3.250(1)	40.7(6)	40
$In^{III}Pc_2$	−1.5	2.333	2.741(9)	42.2(4)	37
$[In^{III}Pc_2](I_3)_{2/3}$	−1.167	2.523	3.196(1)	40.0(4)	43
$TiPc_2$ [a]	−2	2.32	2.32	45	60
$[TiPc_2](I_3)_{2/3}$	−1.667	2.246	2.42	41.1	38

[a] "Stapled" by two C−C σ bonds.

(61) Gieren, A.; Hoppe, W. *J. Chem. Soc., Chem. Commun.* **1971**, 413−414.
(62) Bennett, W. E.; Broberg, D. E.; Baenziger, N. C. *Inorg. Chem.* **1973**, *12*, 930−936.
(63) DeCian, A.; Moussavi, M.; Fischer, J.; Weiss, R. *Inorg. Chem.* **1985**, *24*, 3162−3167.
(64) Ercolani, C.; Paoletti, A. M.; Pennesi, G.; Rossi, G.; Chiesi-Villa, A.; Rizzoli, C. *J. Chem. Soc., Dalton Trans.* **1990**, 1971−1977.
(65) Janczak, J.; Kubiak, R. *J. Alloys Compd.* **1994**, *204*, 5−11.
(66) Shannon, R. D. *Acta Crystallogr., Sect. A* **1967**, *32*, 751−767.

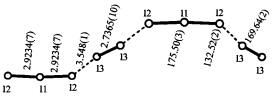

Figure 3. View of the polymer zigzag chain of interacting I_3^- ions with I_2.

both phthalocyaninato rings are "stapled" by two interligand C−C σ bonds. It should be added that oxidation of the $TiPc_2$ complex by iodine leads to the breaking of these interligand C−C σ bonds. Additionally, similar examples of the "stapled" niobium diphthalocyaninato complexes have been recently investigated.[67,68]

In contrast to the well-known tetragonal form of iodine-doped metallophthalocyanines and diphthalocyanines in which the iodine-doped atoms develop linear chains of symmetrical triiodide ions that are disordered (translated) in the crystal, in this $[ZrPc_2]I_3 \cdot I_2$ monoclinic crystal the iodine atoms form polyiodine zigzag chains of ordered symmetric but slightly bent I_3^- ions and neutral diiodine molecules that are bridging the I_3^- ions (see Figure 3). Recently, for the understanding of the bonding in the I_3^- ion, i.e., electron-rich three-center bonding, in more detail, theoretical calculations using qualitative molecular orbital theory have been performed.[69] The $I-I_2$ bonding energy in the symmetric triiodide ions has been calculated to be 37.5 kcal/mol, and the calculated charge gave −0.419 for both terminal iodines and −0.162 on the central I atom. The I−I distance in the symmetrical I_3^- ions is equal to 2.9234(7) Å. The distortion of the I_3^- ion from linear form (the I−I−I angle of 175.50-(3)°) is due to the interaction of negatively charged terminal I atoms with the neighboring bridging neutral I_2 molecules in the chains (Figure 3). The slightly bending character of I_3^- ions can be found in the two isostructural iodine-doped arsenic and antimony phthalocyanines, $AsPcI_3$ and $SbPcI_3$.[70,71] The I−I bond length in the neutral diiodine molecule is comparable to that found in the other structures of metallophthalocyaninato complexes containing a neutral I_2 molecule. For example, the I−I bond length of an I_2 molecule in the crystal of $GePcI_2 \cdot I_2$ is equal to 2.770(2) Å[52] and in $CrPc\ I_2 \cdot I_2$ is equal to 2.773(1) Å,[53] both complexes in which the neutral diiodine molecule is a bridge for developing polymeric structures. In the dimeric structure of $(FePcI)_2I_2$ the I−I bond length in the bridging I_2 molecule is equal to 2.666(2) Å.[51] The I−I distance of 2.736(1) Å of neutral I_2 molecule in the crystal of $[ZrPc_2]I_3 \cdot I_2$ is comparable to that found in the pure iodine in the solid in which the I−I distance is equal to 2.715(6) Å at 110 K,[72] and the I···I distance of 3.548(1) Å between the terminal I of I_3^- ion and the I of I_2 molecule within the polyiodine chains is slightly longer than the intermolecular distance in the pure iodine in which it is

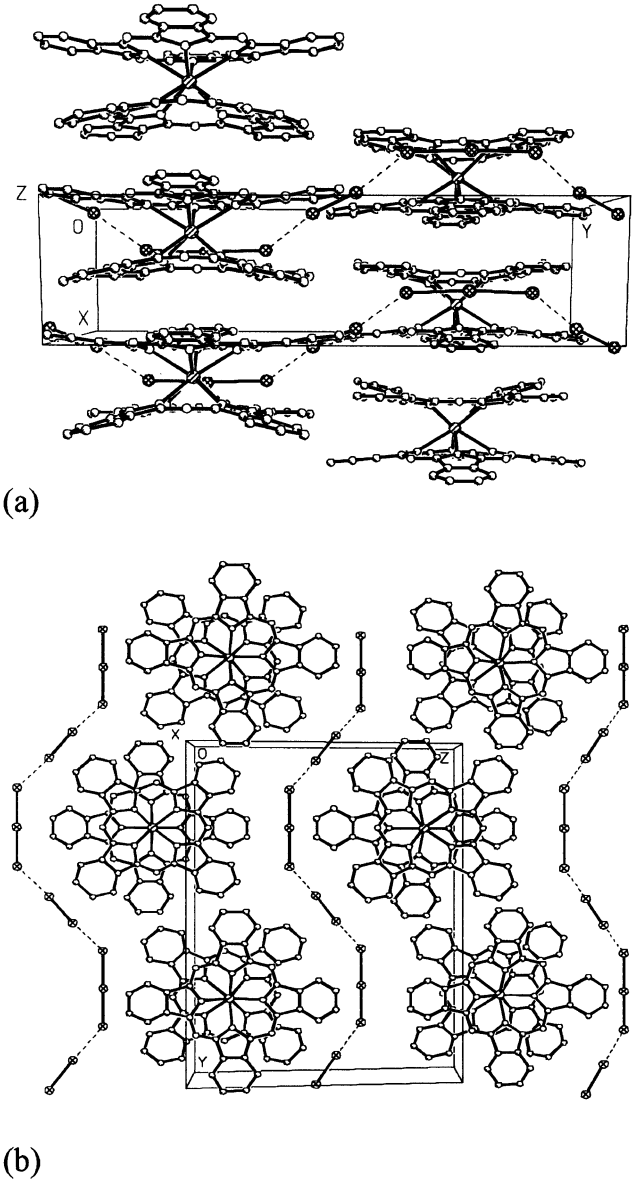

Figure 4. View of the crystal structure of $[ZrPc_2]I_3 \cdot I_2$ (a) perpendicular to the stacks of $[ZrPc_2]^+$ units and (b) along the stacks. H atoms are omitted for clarity.

equal to 3.50 Å[72] and indicates the weak interaction between the I_2 and I_3^- moieties in the chains.

The one-electron-oxidized $[ZrPc_2]^+$ units in the crystal form pseudo-monodimensional columnar stacks. The stacks are aligned along the *a* axis of the crystal (Figure 4), and the mean planes of phthalocyaninato rings are parallel to the *bc* plane. The intermolecular Pc···Pc distances with the average value of ∼3.2 Å between two neighboring $[ZrPc_2]^+$ units indicate the $\pi-\pi$ interaction of the Pc rings. However, due to the saucer-shaped form of Pc rings and the back-to-back orientation between two $[ZrPc_2]^+$ units within the stack, this interaction is weaker in relation to that between Pc rings in the tetragonal iodine-doped metallophthalocyanines, in which the rings are closely planar; thus, the π-clouds interaction between Pc rings is more effective. These interactions are closely related with the conducting properties of these iodine-doped MPc materials.

(67) Donzello, M. P.; Ercolani, C.; Chiesi-Villa, A.; Rizzoli, C. *Inorg. Chem.* **1998**, *37*, 1347−1351.
(68) Janczak, J.; Kubiak, R. *Polyhedron* **2002**, *22*, 313−322.
(69) Landrum, G. A.; Goldberg, N.; Hoffman, R. *J. Chem. Soc., Dalton Trans.* **1997**, 3605−3613.
(70) Kubiak, R.; Janczak, J.; Razik, M. *Inorg. Chim. Acta* **1999**, *293*, 155−159.
(71) Janczak, J.; Idemori, Y, M. *Acta Crystallogr., Sect. E* **2002**, *58*, m36−m38.
(72) Van Bolhius, F.; Kostner, B. P.; Migchelsen, T. *Acta Crystallogr.* **1967**, *23*, 90−91.

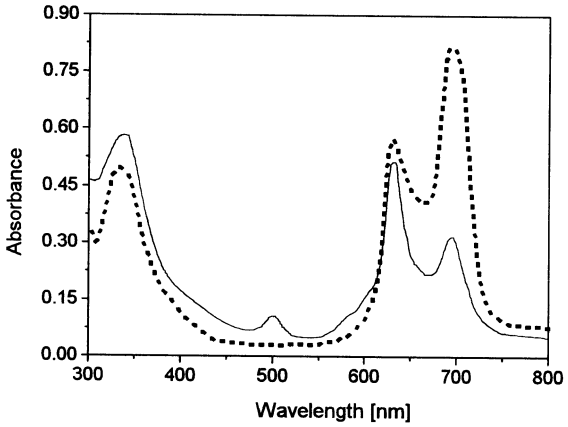

Figure 5. Electronic absorption spectrum of one-electron-oxidized $[ZrPc_2]I_3 \cdot I_2$ (solid line) and nonoxidized $ZrPc_2$ (dashed line).

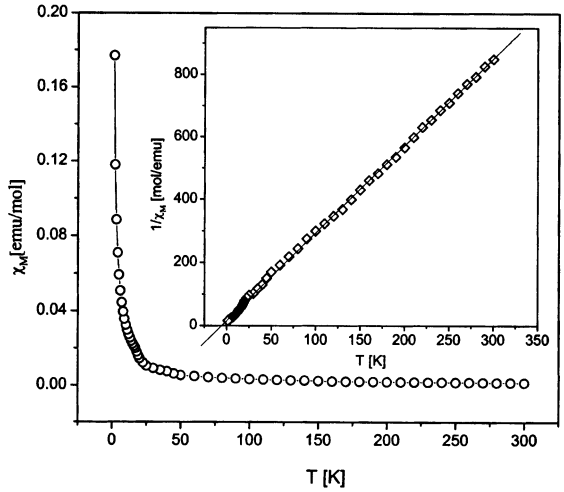

Figure 6. Plots of the χ_M and $1/\chi_M$ of the $[ZrPc_2]I_3 \cdot I_2$ solid sample versus T.

The one-dimensional chains of $\cdots I_3^- \cdots I_2 \cdots (I_3^- \cdots I_2)_n \cdots I_3^- \cdots I_2 \cdots$ in the crystal are located along the *b* axis; thus, both monodimensional aggregates, i.e., the columnar stacks of $[ZrPc_2]^+$ units and polyiodine chains, are perpendicular. This arrangement is different from that observed for the tetragonal form of iodine-doped metallophthalocyaninato or diphthalocyaninato complexes, in which both one-dimensional oppositely charged aggregates, the columnar stack of $[MPc_2^{\delta+}]_n$ and $(I_3^-)_n$, are parallel to each other and aligned along the *c* axis of the tetragonal system.

UV−Vis Spectroscopy. The electronic absorption spectra of both complexes, i.e., unoxidized $ZrPc_2$ and one-electron-oxidized $[ZrPc_2]I_3 \cdot I_2$, are very similar (see Figure 5) which indicates that the interaction between $[ZrPc_2]^+$ and $I_3^- \cdots I_2$ units is insignificant in the positions of the phthalocyanine's HOMO and LUMO levels. The Q-band corresponds to the excitation from HOMO (a_{1u}) to LUMO (e_g) while the B-soret band is mostly an $a_{2u} \rightarrow e_g$ transition. The Q-band splits into two bands at 696 and 635 nm in $ZrPc_2$ and 698 and 632 nm in oxidized $[ZrPc_2]I_3 \cdot I_2$. These values correspond to the range of 1.96−1.77 eV that correlate well to the difference between the first oxidation and first reduction potential of the $ZrPc_2$ complex.[58] The splitting values of 61 nm in $ZrPc_2$ and 66 nm in $[ZrPc_2]I_3 \cdot I_2$ result from the vibronic coupling in the excited state.[73−77] Several authors reported that the splitting value of the Q-band decreases as the interplanar Pc−Pc distance increases.[76,77] Additionally, Takahashi et al. reported that if the interplanar Pc−Pc distance increases, the intensity of the Q_2 band decreases and that of Q_1 increases.[78] The inversion of the intensities of the Q_1 and Q_2 bands and the splitting values in the spectrum of $ZrPc_2$ and $[ZrPc_2]I_3 \cdot I_2$ are fully consistent with the X-ray single-crystal analysis (the interplanar distance of 2.494(3) Å in $[ZrPc_2]I_3 \cdot I_2$ is shorter than in $ZrPc_2$ (2.52 Å)). In the spectrum of $[ZrPc_2]I_3 \cdot I_2$ besides these two characteristic bands (B and Q) observed in the spectrum of unoxidized $ZrPc_2$ one additional band at ∼502 nm is observed. This band is evidence for the existence of the one-electron-oxidized phthalocyaninato(−) radical ligand and is assigned to the electronic transition from a deeper level to the half-occupied HOMO level. A similar band has been observed in the spectrum of other one-oxidized metallophthalocyaninato complexes, such as $Lu^{III}Pc_2$ or $In^{III}Pc_2$.[79,80]

Magnetic Properties. The magnetic susceptibility of $[ZrPc_2]I_3 \cdot I_2$ was measured between 300 and 1.8 K. The paramagnetic susceptibility was obtained by subtracting the temperature-independent diamagnetic contribution of the phthalocyaninato rings and diamagnetism of the closed-shell (d^0) Zr^{4+} cation. The value of the diamagnetic contribution for the I_3^- and I_2 was calculated from Pascal's constants.[81,82] The corrected paramagnetic susceptibility of $[ZrPc_2]I_3 \cdot I_2$ at 300 K is $\approx 1.18 \times 10^{-3}$ emu mol^{-1}. This value corresponds to ∼0.96 spins/molecule ($S = 1/2$, $g \cong 2$). The temperature dependence of the corrected magnetic susceptibility $[ZrPc_2]I_3 \cdot I_2$ can be fit approximately by the Curie−Weiss law, $\chi_M = C/(T - \Theta)$, with the Weiss constant Θ (K) of ≈−3.9 (see Figure 6). The negative Weiss constant represents the antiferromagnetic coupling among unpaired electrons.

The EPR spectrum measured on the solid-state samples of $[ZrPc_2]I_3 \cdot I_2$ at room temperature exhibits one rather narrow signal in proximity of the free electron *g* value. The *g* value of 2.0026 and $\Gamma = 6.2$ G indicate the formation of a ligand-centered π-radical. As shown in the X-ray single-crystal analysis of $[ZrPc_2]I_3 \cdot I_2$, the two phthalocyaninato ligands are quite similar in bond lengths and angles. It is once again noticed here that the oxidation of $ZrPc_2$ by iodine is ligand-

(73) Henrikson, A.; Roos, B.; Sundon, R. *Theor. Chim. Acta* **1972**, *27*, 303−309.
(74) Lee, L. K.; Sabelli, N. H.; Leberton, P. R. *J. Phys. Chem.* **1982**, *86*, 3926−3931.
(75) Shiari, H.; Tsuiki, H.; Masuda, E.; Koyama, T.; Hanabusa, K.; Kobayashi, N. *J. Phys. Chem.* **1991**, *95*, 417−423.
(76) Ishikawa, N.; Kaizu, Y. *J. Phys. Chem.* **1996**, *100*, 8722−8730.
(77) Takahashi, K.; Tomita, Y.; Harada, Y.; Tsubota, K.; Honda, M.; Kasuga, K.; Sogabe, K.; Tokii, T. *Chem. Lett.* **1992**, 759−760.
(78) Takahashi, T.; Shimoda, J.; Itoch, M.; Fuchita, Y.; Okawa, H. *Chem. Lett.* **1998**, 173−174.
(79) Orti, E.; Bredas, J. E.; Clarisse, C. *J. Chem. Phys.* **1990**, *92*, 1228−1235.
(80) Janczak, J. *Pol. J. Chem.* **1998**, *72*, 1871−1878.
(81) Earnshaw, A. In *Introduction to Magnetochemistry*; Academic Press: London, 1968; pp 4−8.
(82) Mulay, L. N. In *Theory and Applications of Molecular Diamagnetism*; Mulay, L. N., Boudreaux, E. A., Eds.; Wiley-Interscience: New York, 1976; Chapter 5.3.

centered and homogeneously affecting both phthalocyaninato ligands; thus, the nonintegral formal oxidation state (−1.5) should be assigned to both of them. The *g* value observed in the EPR spectrum of $[ZrPc_2]I_3{\cdot}I_2$ is the same as observed for the other partially oxidized tetragonal form $[ZrPc_2](I_3)_{2/3}$ [43] and comparable with the *g* value observed in the EPR spectrum of other partially oxidized closed-shell metallodiphthalocyaninato complexes; for example, in $In^{III}Pc_2$ (In^{3+}, d^{10} configuration) the $g = 2.0025$[37] and in $[In^{III}Pc_2](I_3)_{2/3}$ the $g = 2.0028$.[43] The calculation of the spin concentration yields 3.165×10^{20} spins/g (∼0.92 unpaired electron/$[ZrPc_2]I_3{\cdot}I_2$ molecule). The spin concentration obtained from EPR is in good agreement with the magnetic susceptibility measurements. The spin concentration in $[ZrPc_2]I_3{\cdot}I_2$ is greater than the calculated one from EPR measurement of the tetragonal form $[ZrPc_2](I_3)_{2/3}$.[43] The difference of the spin concentration between the $[ZrPc_2]I_3{\cdot}I_2$ (monoclinic) and $[ZrPc_2](I_3)_{2/3}$ (tetragonal) results from the difference in their crystal structures. In the tetragonal crystal of $[ZrPc_2](I_3)_{2/3}$ the phthalocyaninato ligands are closely planar, so the interactions between the $Pc^{\bullet-}$ radicals are more effective and lead to the decreasing of the calculated spin concentration in relation to the monoclinic $[ZrPc_2]I_3{\cdot}I_2$ crystals in which the $\pi-\pi$ interactions are less effective due to the saucer-shaped phthalocyaninato rings.

Single-Crystal Electrical Conductivity. The conductivity of $[ZrPc_2]I_3{\cdot}I_2$ measured on single crystal along the *a* crystallographic axis, i.e., along the stacking axis of one-electron-oxidized $[ZrPc_2]^+$ units (see Figure 4a), is equal to 3.8 Ω^{-1} cm^{-1}, while measured along the *b* axis, i.e., perpendicular to the $[ZrPc_2]^+$ stacks but along the zigzag polymer of interacting iodine species $\cdots I_3^- \cdots I_2 \cdots I_3^- \cdots I_2^- \cdots$ (see Figure 4b), is equal to $\sim 2.1 \times 10^{-3}$ Ω^{-1} cm^{-1} at room temperature. For the other partially oxidized by iodine zirconium diphthalocyanine $[ZrPc_2](I_3)_{2/3}$ complex (tetragonal form), the conductivity data are available only on a polycrystalline sample;[43] therefore, for this $[ZrPc_2]I_3{\cdot}I_2$ monoclinic form the conductivity measurement was also made on polycrystalline sample, for a comparison. The conductivity on the polycrystalline sample of $[ZrPc_2]I_3{\cdot}I_2$ pressed into pellets ($\sim 10^5$ kPa) is equal to $(5.5-6.2) \times 10^{-2}$ Ω^{-1} cm^{-1} and is slightly greater than the conductivity of $[ZrPc_2](I_3)_{2/3}$ ($(5.2-5.5) \times 10^{-2}$ Ω^{-1} cm^{-1}).[43] The conductivity of unoxidized $ZrPc_2$ measured on polycrystalline material at room temperature shows typical values for isolators ($\sigma_{RT} < 10^{-9}$ Ω^{-1} cm^{-1}).

The single-crystal conductivity along the stacks of $[ZrPc_2]^+$ units decreases with decreasing temperature (Figure 7a); thus, the crystal exhibits nonmetallic character in conductivity ($d\sigma/dT > 0$). Generally a nonmetallic molecular conductor exhibits an exponential temperature dependence of $\sigma(T)$, because the carrier density or mobility or both are activated. The temperature dependence of conductivity may be fit by the expression $\sigma = \sigma_0 \exp(-E_a/kT)$, where E_a is the activation energy and *k* is Boltzman's constant. A least-squares fit to the data ($\ln(\sigma/\sigma_{RT})$ vs $1000/T$; see Figure 7b) yields activation energy of 0.025 eV. The relatively high conductivity of this sandwich-type diphthalocyaninato complex $[ZrPc_2]I_3{\cdot}I_2$ along

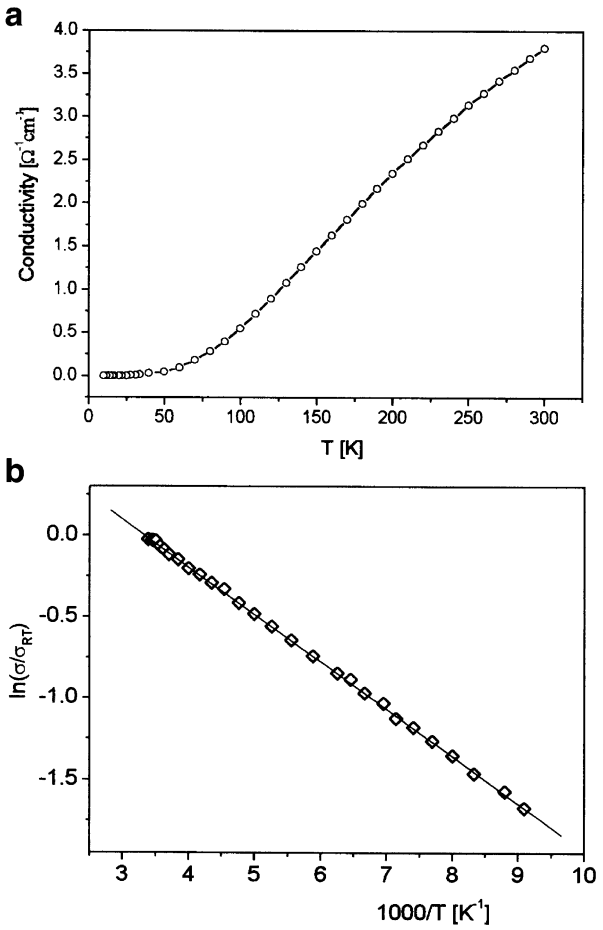

Figure 7. (a) Temperature dependence of the conductivity of $[ZrPc_2]I_3{\cdot}I_2$ measured along the *a* crystallographic axis, i.e., along the stacks of $[ZrPc_2]^+$ units, and (b) $\ln(\sigma/\sigma_{RT})$ vs $1000/T$.

the stacks of $[ZrPc_2]^+$ units but significantly lower in comparison to the conductivity of the NiPcI ($\sigma_{RT} \sim 600$ Ω^{-1} cm^{-1}), the first molecular conductor,[15] can be explained by a significant overlap of the ligand π-orbitals resulting from the staggering orientation of the Pc rings (rotation angle equals 45.0(2)° in the sandwich $ZrPc_2$ as well as between the sandwich within the stack). This rotation makes short the eight inter-ring contacts between the pyrrole α-carbon atoms (the inter-ring $C_\alpha \cdots C_\alpha$ contacts ranging from 2.839(3) to 3.024(3) Å). These carbon atoms make appreciable contributions to the partially occupied HOMO π-molecular orbital of the Pc macrocycle (the great overlap of the HOMO Pc orbitals) that form a conduction band of partially oxidized crystals. A similar nonmetallic character in conductivity ($d\sigma/dT > 0$) is observed along the *a* axis (along the polymer zigzag chains of weakly interacting I_3^- ions and neutral I_2 molecules) as illustrate Figure 8, but the conductivity in this direction is lower by a factor of $\sim 10^3$.

These data clearly show that the charge propagation mainly proceeds along the one-dimensional $[ZrPc_2]^+$ stacks as illustrated in Scheme 3a. During the charge transport there is no need to change the population distribution among the sites, since the crystal of iodine-doped diphthalocyaninato complex with closed-shell (d^0) Zr^{4+} cation contains a partially oxidized phthalocyaninato macroring, as evidenced by EPR spectroscopy. Each one-electron-oxidized $[ZrPc_2]^+$ unit

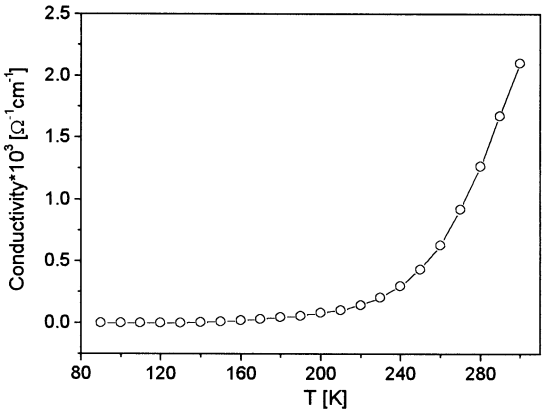

Figure 8. Temperature dependence of the conductivity of $[ZrPc_2]I_3 \cdot I_2$ measured along the *b* crystallographic axis, i.e., along the interacting I_3^- ions and neutral I_2 molecules.

contains Pc^{2-} and one-electron-oxidized $Pc^{\bullet -}$ radical ligand; thus, the jumping of the electron from one side to another with the preformed hole takes place between isoenergetic configurations (see Scheme 3a). This is consistent with the relatively low activation energy (0.025 eV) obtained by the fit of the conductivity data. In the tetragonal crystals of $[ZrPc_2](I_3)_{2/3}$, the charge transfer along the stacks of $[ZrPc_2]^{2/3+}$ is less effective since statistically one of three $ZrPc_2$ units contains two Pc^{2-} ligands, in contrast to the monoclinic crystals of $[ZrPc_2]I_3 \cdot I_2$, where each $[ZrPc_2]^+$ unit contains both Pc^{2-} and $Pc^{\bullet -}$ ligands. As it is shown in the Scheme 3b, the charge transport in a nonoxidized molecular system, as for example the $ZrPc_2$ (see Scheme 3b, left stack), requires a large activation energy for a carrier creation, since this involves a high energy of states with separated positive and negative ions along the chain (see Scheme 3b, right stack). The activation energy is comparable to the sums of the energies that are related to the one-electron oxidation and one-electron reduction of the $ZrPc_2$ complex and the formation of the $[ZrPc_2]^+$ and $[ZrPc_2]^-$ ions. The first oxidation and the first reduction peaks obtained by a cyclic voltammetry on $ZrPc_2$ are observed at +1.2 and −1.4 V, respectively.[59]

Scheme 3

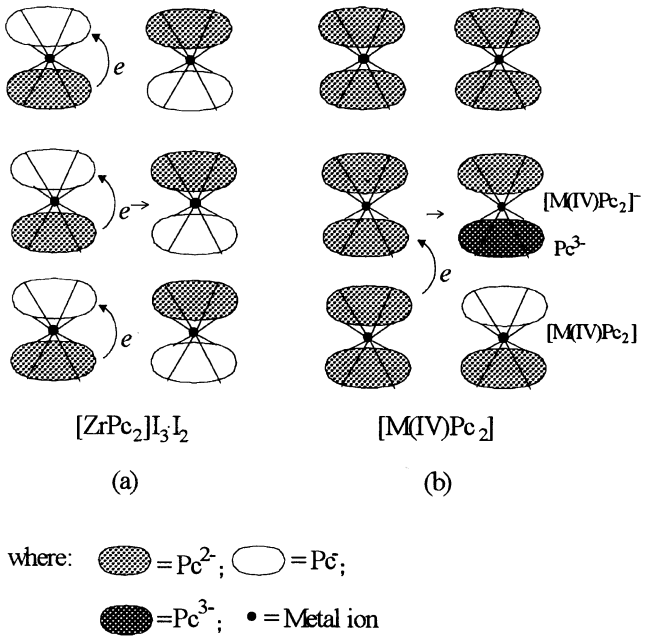

Acknowledgment. This work was supported by a grant (No. 3 T09A 180 19) from the Polish State Committee for Scientific Research.

Supporting Information Available: An X-ray crystallographic file in CIF format. This material is available free of charge via the Internet at http://pubs.acs.org.

IC020717I